Investigating the feedback between CO2, vegetation and the AMOC in a coupled climate model

Climate Dynamics
https://doi.org/10.1007/s00382-019-04634-2

Investigating the feedbacks between CO_2, vegetation and the AMOC in a coupled climate model

Edward Armstrong[1] · **Paul Valdes**[1] · **Jo House**[1] · **Joy Singarayer**[2]

Received: 31 January 2018 / Accepted: 16 January 2019

Abstract
The Atlantic Meridional Overturning Circulation (AMOC) is an important component of the climate system, however its sensitivity to the terrestrial biosphere has been largely overlooked. Here the HadCM3 coupled climate model is run for millennial timescales to investigate the feedbacks between vegetation and the AMOC at increasing CO_2. The impact of agricultural conversion (termed land-use change; LUC) and the role of the simulated 'background' vegetation (termed land cover change; LCC) are investigated. LUC cools climate in regions of high crop fraction due to increased albedo. LCC is shown to evolve at higher CO_2, with a northward migration of the tree line in the Northern Hemisphere and dieback of the Amazon. This generally acts to enhance the impact of climate change primarily due to albedo changes. Density in the Greenland-Iceland-Norwegian (GIN) Seas is crucial in driving the AMOC. Increasing CO_2 decreases regional sea surface density, reducing convection and weakening the AMOC. The inclusion of LCC is shown to be responsible for a significant proportion of this weakening; reflecting the amplification effect it has on climate change. This acts to decrease the surface density in the GIN Seas. At elevated CO_2 (1400 ppm) the inclusion of dynamic vegetation is shown to drive a reduction in AMOC strength from 6 to 20%. Despite the cooling effect of LUC, the impact on the AMOC is shown to be small reflecting minimal impact it has on GIN Sea density. These results indicate the importance of including dynamic vegetation in future AMOC studies using HadCM3, but LUC may be insignificant. In the context of other climate models however, the importance of vegetation is likely to be overshadowed by other systemic model biases.

1 Introduction

The Atlantic Meridional Overturning Circulation (AMOC) has a significant impact on regional and global climate. However there remains considerable uncertainty between models regarding its response to future climate changes. Determining its sensitivity to a range of model variables is crucial in order to understand the mechanisms that dictate AMOC strength and variability, and how they may respond to a changing climate.

Past work has focused predominantly on how the strength of the AMOC may be influenced by increasing CO_2. Many of these have shown that an increase in CO_2 and consequent warming in key sites of convection such as the Greenland-Iceland-Norwegian (GIN) Seas and/or Labrador Sea would reduce the surface density of water via changes in freshwater flux and/or surface heat loss and consequently weaken the AMOC (e.g. Gregory et al. 2005; Swingedouw et al. 2007; Thorpe et al. 2001; Dixon et al. 1999; Mikolajewicz and Voss 2000; Bakker et al. 2016; Armstrong et al. 2017).

There remain a number of research areas that have been largely excluded from past AMOC studies. One such example is the sensitivity of the AMOC to the terrestrial biosphere, such as the distribution of vegetation used in climate models. Vegetation alters the land surface structure and impacts biogeophysical processes including albedo, moisture fluxes and leaf-area index (LAI). This consequently influences the surface energy balance, the partitioning of latent and sensible heat and shortwave radiation reaching the surface (Bala et al. 2007; Boisier et al. 2012; Brovkin et al. 2009; Pielke et al. 2002). Such changes might have an influence on the AMOC.

The distribution and physiology of natural vegetation is expected to change with increasing concentrations of

✉ Edward Armstrong
edward.armstrong@bristol.ac.uk

[1] School of Geographical Sciences, University of Bristol, University Road, Bristol BS8 1SS, UK

[2] Department of Meteorology, Centre for Past Climate Change, University of Reading, Bristol, UK

Published online: 01 February 2019

CO_2, with northward migration of the treeline and possible spread of deciduous woodland in place of needleleaf. Mapping such changes in climate models employs the use of a dynamic global vegetation model (DGVM), which simulates vegetation depending on a range of parameters including temperature, water and carbon. These changes consequently alter the biogeophysical fluxes from the land surface, generating a range of positive or negative feedbacks that can act to either attenuate or amplify climate change depending on the location. This shift in vegetation distribution is referred to here as land-cover change (LCC).

Simulating crops in place of 'natural' vegetation in a climate model has also been shown to impact regional and global climate (Armstrong et al. 2016; Bathiany et al. 2010; Bonan 2001; Claussen et al. 2001; Ge 2010), a process here termed land-use change (LUC). The response of the climate to LUC varies depending on the spatial scale and the latitude at which it occurs, with tropical LUC shown to drive a warming impact and temperate LUC potentially causing a regional cooling effect (Bathiany et al. 2010; Claussen et al. 2001; Snyder et al. 2004).

Past studies that have investigated the feedbacks between vegetation and the AMOC have primarily focused on the way in which large-scale AMOC changes influence vegetation distribution. These include potential abrupt shifts following the Dansgaard–Oeschger (D-O) and Heinrich (HE) events, which have been hypothesised to be driven by rapid AMOC fluctuations (Allen et al. 1999; Fletcher et al. 2010; Grimm et al. 2006; Woillez et al. 2013). However there has been less of a focus on how sensitive the AMOC is to LUC and LCC and how this may change at higher CO_2. Despite the potentially important role vegetation plays in the climate system it is commonly kept static in climate modelling studies, such as those included in the CMIP3 and CMIP5 experiments (Jiang et al. 2011). It is therefore important to better constrain if and to what extent the AMOC is sensitive to LCC and LUC at increasing CO_2, in order to gain an understanding of the importance of including dynamic vegetation and/or crops when simulating the AMOC.

This study aims to answer this question in the context of increasing concentrations of CO_2 using millennial simulations of the HadCM3 coupled climate model. Simulations are run at four quasi-equilibrium CO_2 concentrations and coupled with the DGVM TRIFFID, different LCC distributions and a crop mask (LUC). Section 2 outlines the model and methods, Sect. 3 gives an overview of the model climatology and the impact of CO_2, LUC and LCC on the GIN Seas region. Section 4 investigates the impact of CO_2, LUC and LCC on the AMOC, and Sect. 5 examines the impact of the AMOC on LCC. A discussion and summary is given in Sect. 6.

2 Methods

2.1 The HadCM3 model

The Hadley Centre model version 3 (HadCM3) is a coupled climate model consisting of a dynamical atmosphere model (HadAM3, Pope et al. 2000) and ocean model (HadCOM3, Gordon et al. 2000). Despite the relatively old age of HadCM3, the model has been shown to produce an accurate representation of different climate variables (Flato et al. 2013; Valdes et al. 2017). A key advantage of the model is that it is computationally fast, which permits long (i.e. millennial) scale simulations beneficial for investigating modes of internal variability. A detailed description of the version of HadCM3 used in this study, and an overview of minor bug fixes from the original model code are given in Valdes et al. (2017).

In this study HadCM3 incorporates the land-surface scheme MOSES version 2.1 (Met Office Surface Exchange Scheme version 2.1) (Essery et al. 2003; Valdes et al. 2017). MOSES models the fluxes of energy and water, including the physiological processes of transpiration, respiration and photosynthesis. It is coupled with the DGVM TRIFFID, and simulates the fractional coverage of nine different surface types on a sub-grid scale. These include five plant functional types (PFTs): broadleaf trees, needleleaf trees, shrubs, C3 (temperate) grasses and C4 (tropical) grasses, and four non-vegetated types: urban, inland water, bare soil, and ice. Excluding ice type, each land-surface gridbox can be made up of any mixture of the other eight surface types.

Each of the PFTs has a different value for a range of phenological characteristics including LAI, albedo and maximum canopy interception. The PFT therefore plays a crucial role in TRIFFID, not only determining the structural characteristics of each grid box, but also the ecological processes that occur (i.e. rooting depth, stomatal conductance, LAI, etc.). They are simulated dynamically by TRIFFID based on a competitive hierarchy, where trees displace shrubs that in turn displace grasses (i.e. trees > shrubs > grasses). TRIFFID produces the vegetation coverage, canopy height and LAI according to the net carbon fluxes that are simulated by MOSES. The surface energy balance is explicitly solved in each gridbox, with the fraction of a surface type determining how much that type contributes to the overall land gridbox surface properties.

In Valdes et al. (2017), HadCM3 is shown to represent key components of the climate accurately and rembains competitive to other, more modern, climate models (see their Fig. 2). There are however a number of drawbacks that might impact the simulation of the AMOC. Firstly

AMOC peak flow is at 800 m depth in HadCM3 (see Fig. 8 in Valdes et al. 2017), shallower than the 1000 m observed by the RAPID Array (Smeed et al. 2015). In the oceans, limits to resolution impact some oceanic overflow channels such as those in the North Atlantic region, resulting in an artificial deepening of the Greenland-Scotland Ridge and Denmark Straits (Roberts et al. 1996; Gordon et al. 2000) and closure of the Canadian Archipelago. There is no net volume transport through the Bering Straits, which is not consistent with observations and may influence the AMOC (Hu and Meehl 2005; Cattle and Cresswell 2000). Finally a weaker than observed wind stress might impact Gyre formation in the North Atlantic (Gordon et al. 2000).

Table 1 Overview of simulations used in this study

Experiment name	CO_2 (ppm)	Key points
Base simulations		
1x	350	Dynamic vegetation
2x	700	Dynamic vegetation
3x	1050	Dynamic vegetation
4x	1400	Dynamic vegetation
LUC simulations		
1xLU	350	Dynamic vegetation with crop mask
2xLU	700	Dynamic vegetation with crop mask
3xLU	1050	Dynamic vegetation with crop mask
4xLU	1400	Dynamic vegetation with crop mask
noLCC simulations		
1x_4xVEG	350	Static vegetation. Vegetation distribution at 4x CO_2 initiated from the end of 4x
4x_1xVEG	1400	Static vegetation. Vegetation distribution at 1x CO_2 initiated from the end of 1x

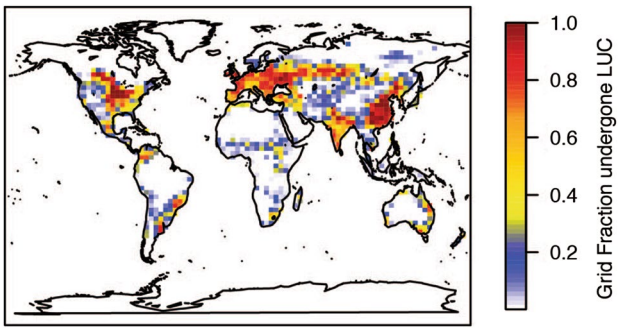

Fig. 1 The proportion of each grid square in HadCM3 that has been subject to land use change, i.e. the replacement of natural vegetation simulated by TRIFFID with C3 or C4 grasses. Based on the land cover mask of Betts et al. (2007)

2.2 Experimental set-up

This study is based on 10, 2000 year simulations of HadCM3, split into three groups; 'base', 'LUC' and 'noLCC' (Table 1). The base simulations are quasi-equilibrium model runs with dynamic TRIFFID at four CO_2 concentrations; 350, 700, 1050 and 1400 ppm. The 1400 ppm scenario is approximate to that estimated by the year 2150 under the IPCC representative concentration pathway (RCP) 8.5 (Meinshausen et al. 2011), the most extreme emissions trajectory forecast by the IPCC. We will refer to these experiments as 1x, 2x, 3x and 4x respectively.

TRIFFID does not incorporate a dynamic LUC element, so global LUC is simulated using a crop/pasture mask originally from the study of (Betts et al. 2007) and shown in Fig. 1. This replaces simulated natural vegetation with C3 and C4 grasses or bare soil, representing crop and pasture values for the year 1990 derived by Ramankutty and Foley (1999) and (Goldewijk 2001) respectively. This mask does not vary with time and is kept constant for each CO_2 concentration. Although this is a relatively simplistic approach, it permits direct comparison of the LUC runs. Simulations were run at the same four CO_2 concentrations and are hereon labelled 1xLU, 2xLU, 3xLU and 4xLU.

In order to investigate the impact of excluding a dynamic LCC component in the model, two further simulations were run with altered 'natural' vegetation distribution, here termed 1x_4xVEG and 4x_1xVEG. The dominant PFTs simulated by TRIFFID at the end of the 1x and 4x simulations are shown in Fig. 2. Increasing concentrations of CO_2 drive a significant change in vegetation distribution, in response to four factors; available carbon, moisture, temperature and atmospheric CO_2 (Cox 2001). Changes include a northward shift in the tree line across northern Eurasia and North America, a change from deciduous forest to grassland in Africa and grass to bare soil in Australia, and a dramatic die-back of the Amazon region as first identified in (Betts et al. 2004). For the noLCC simulations the background vegetation has been switched; with the 1x_4xVEG simulation being run at 1x CO_2 but with the 4x CO_2 vegetation distribution as shown in Fig. 2. The opposite is the case for the 4x_1xVEG simulation. In both cases, TRIFFID has been switched off to stop vegetation reverting back to its 'natural' state.

For all simulations, analysis is conducted on the final 1000 years in order to allow for a 1000-year spin up of the deep ocean. In order to highlight the equilibrium state of the simulations, Fig. 3 shows the timeseries of the AMOC index (MOI; mean AMOC strength between 40 and 50°N at 800 m). The base and noLCC simulations appear to have reached a quasi-equilibrium state after 1000 years, however a small trend remains in the 2xLU, 3xLU and 4xLU simulations. In order to remove the slight climate drift, the

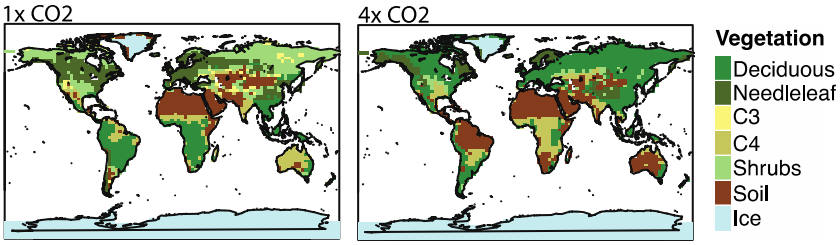

Fig. 2 Maps showing the dominant plant functional types simulated by TRIFFID at the end of the 2000 year base simulations for 1x and 4x CO_2

climate variables, including the streamfunction and MOI as shown in Fig. 3, have subsequently been detrended by subtracting a linear least squares fit.

The moving block bootstrap technique (Wilks 1997) has been used to calculate statistical significance; with a 95% confidence limit applied using the bootstrap percentile method (Hall 1988).

3 The climatology of HadCM3

Figure 4 shows the model climatologies and anomalies for four variables key for the base, LUC and noLCC simulations. The simulations used to calculate the anomalies are shown in each panel and outlined in Table 1.

Higher CO_2 is associated with an increase in SATs with warming focused over land and in the Arctic region, likely a response to the ice-albedo feedback (e.g. Manabe and Stouffer 1980). Precipitation changes are more complex with a broad intensification and a northward shift in the ITCZ. Sea-surface temperatures increase with almost total global coverage with enhanced warming in around the Northern extra tropics and a region to the north of Scandinavia. The mixed layer depth, a key metric in determining the level of convection, shows the deepest region of overturning in the GIN Seas region of up to 250 m at 1x, which shallows by up to 90 m at 4x.

The impact of LUC in HadCM3 is discussed in detail in the study of Armstrong et al. (2016). LUC acts to cool regional climate in areas of high crop fraction, a response to an increase in surface albedo due to replacement of predominantly trees with grasses. Annual global cooling is on the order of −0.31 °C, −0.31 °C, −0.29 °C and −0.26 °C for 1x to 4x CO_2. The seasonal and regional impacts are greater, increasing to −1.43 °C for European summers (see Armstrong et al. 2016 for detailed analysis). There is a small increase in precipitation in regions of cooling likely due to an increase in relative humidity, and a decrease across India that may be a response to a negative feedback with the monsoon hydrological cycle (Singarayer et al. 2009; Singarayer and Davies-Barnard 2012). The impact on the oceans is smaller, with a slight decrease in SSTs predominantly focused in the Northern Hemisphere and only minimal impact to the MLD, which shows a slight deepening at 1x but shallowing at higher CO_2.

The 4x_1xVEG-4x plots show the anomaly when using a 1x vegetation distribution (as shown in Fig. 2) but run at a 4x CO_2 concentration, i.e. the climate impact of not including a dynamic LCC component that is altered by CO_2. There is a cooling across much of the Northern Hemisphere, likely

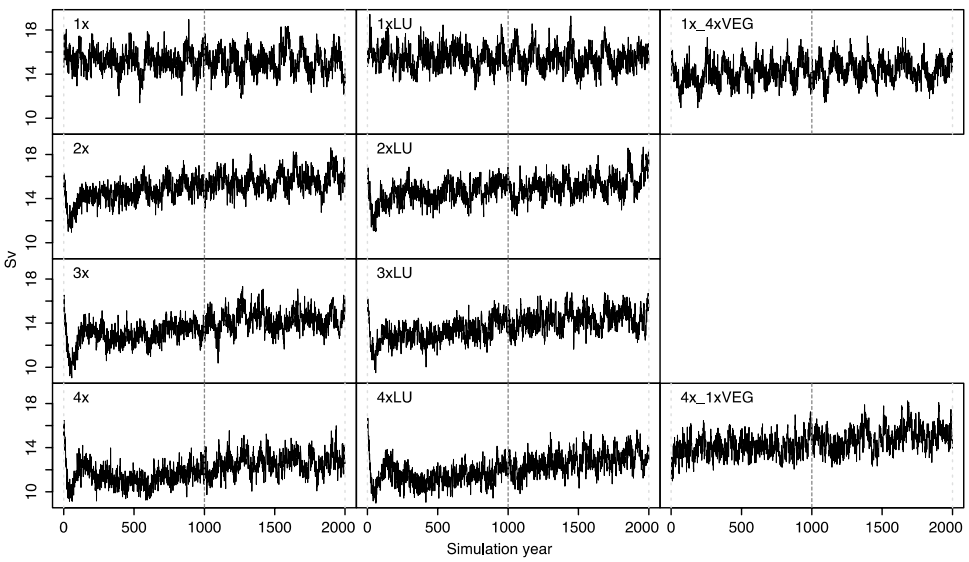

Fig. 3 Full length AMOC Index (MOI) timeseries for the base, LUC and noLCC simulations. The AMOC index is defined as the mean annual strength of the AMOC between 40°N and 50°N at 800 m. The final 1000 years of each simulation, as highlighted with a dashed line, are used in this study and have subsequently been detrended by subtracting a linear least squares fit

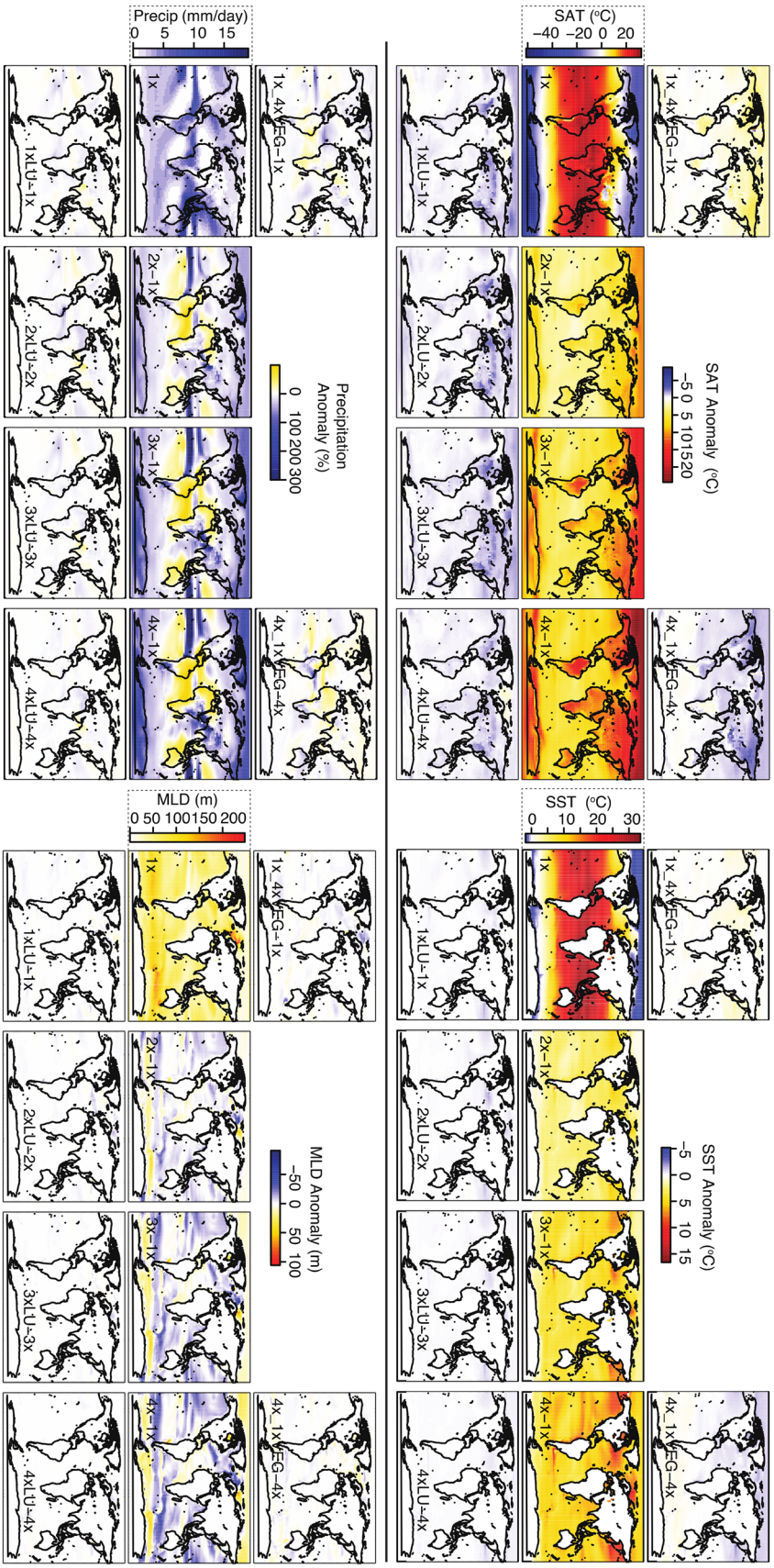

Fig. 4 Mean annual climatology at 1x CO_2 (left central map) and anomalies due to CO_2 in the central panels, LUC (i.e. the conversion of natural vegetation to crops) in the lower panels and noLCC in the top panels. Surface air temperatures (SATs), sea surface temperatures (SSTs), the mixed later depth (MLD) and precipitation are shown clockwise from top left. Only anomalies that are considered 95% confident are shown

due to an increase in albedo from the replacement of forest with shrubs and grasses (see Fig. 2). This cooling may act to reduce relative humidity and so decrease regional precipitation and shift the ITCZ southward in the Atlantic region. The re-introduction of deciduous forest in the Amazon drives a cooling, likely a response to increased evaporation, precipitation, and consequently latent cooling. The cooling impact is also present across the oceans, with a deepening in the MLD of up to 50 m in areas of the GIN Sea. The anomaly pattern for the 1x_4xVEG-1x simulations shows a broadly opposing pattern of change. These anomalies indicate that the dynamic evolution of vegetation with increasing CO_2, specifically the shift in vegetation distribution, significantly impacts climate; acting to amplify warming at higher latitudes likely due to albedo changes, whilst attenuating warming in some regions across the tropics due to both albedo and changes in the hydrological cycle.

3.1 The impact on the GIN seas

Previous studies using HadCM3 (Jackson and Vellinga 2013; Hawkins and Sutton 2007; Vellinga and Wu 2004; Armstrong et al. 2017) have identified that density in the GIN Seas region is crucial in determining the strength and variability of the AMOC. Depth profiles for the region (Fig. 5) demonstrate that fresher, cooler and less dense waters overlie saltier, warmer and denser water. This is likely to reflect cold southerly flow from the East Greenland Current (EGC) sitting above warm north-easterly flow from the North Atlantic Current (NAC). Increasing CO_2 acts to increase temperature throughout the water column, whilst a decrease in surface salinity is contrasted by an increase in the subsurface. These salinity changes might be due to increased precipitation in the Arctic region and so a fresher EGC, whilst there is a saltier inflow via the NAC. These changes show that CO_2 acts to decrease density in the water column and increase stratification.

Both LUC and noLCC are shown to alter the GIN Sea profiles. The anomaly at 4x_1xVEG-4x shows a decrease in potential temperatures of up to 0.7 °C to approximately 1300 m. The anomaly is greater in surface waters; possibly due to the large cooling across the Arctic at 4x_1xVEG that forms this water mass. The anomaly in the full temperature depth profile indicates a decrease in stratification in the GIN Seas. The impact on salinity is minimal at the surface but increases at depth, which in contrast to temperature indicates an increase in stratification. Overall there is an increase in density in the GIN Sea water profile, and despite the conflicting changes in salinity and temperature, a decrease in stratification throughout the whole water column, with a change in density of 2.28 kg m^{-2} for 4x compared to 2.15 kg m^{-2} for 4 × 1xVEG. The decrease in stratification in the top

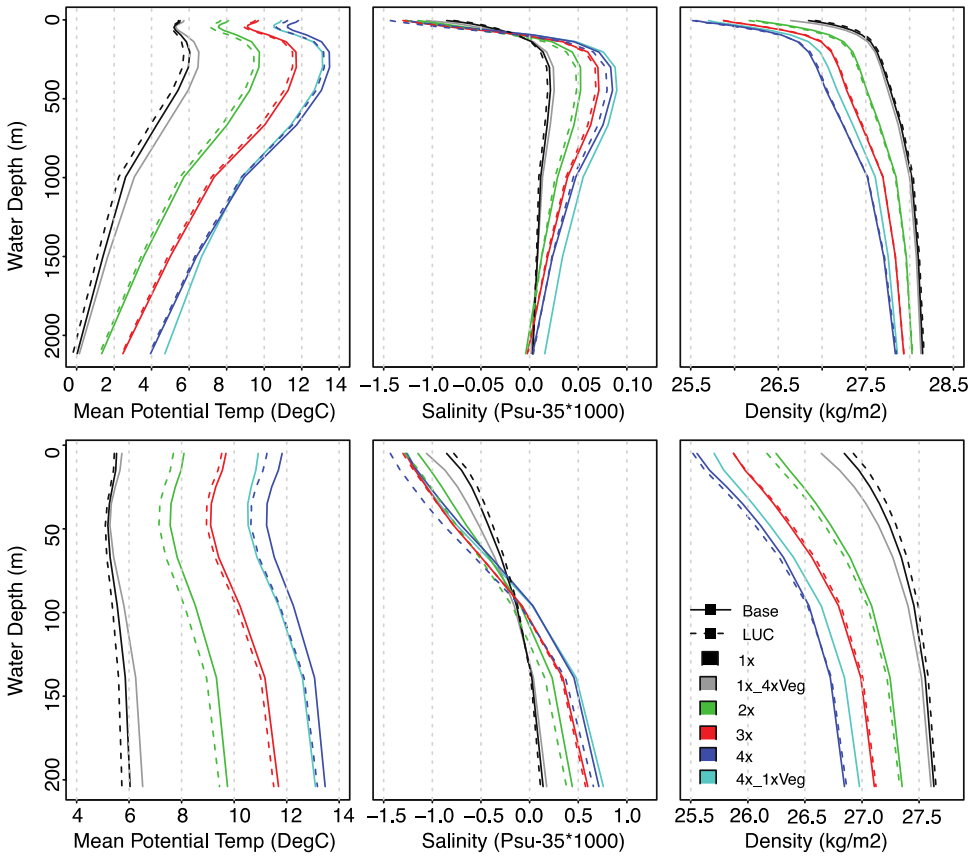

Fig. 5 Mean depth profiles for potential temperature, salinity and density in the GIN seas for all simulations. The top panels show the full depth profile and the bottom panels the top 200 m. The GIN Seas region is defined as 60.625°N–79.375°N: 15°W–10°E

200 m is smaller albeit still present, with a change in density of 1.29 kg m^{-2} for 4x decreasing to 1.27 kg m^{-2} for the 4×1xVEG simulation.

The anomaly at 1x_4xVEG-1x shows an increase in temperature, a decrease in salinity at the surface and increase at depth, resulting in a decrease in density and increase in stratification. This is indicated by a change in density of 1.30 kg m^{-2} for 1x, which increases to 1.49 kg m^{-2} for 1×4xVEG across the 2000 m water column. In the top 200 m, the density change is 0.78 kg m^{-2} for 1x, which increases to 0.96 kg m^{-2} for 1×4xVeg.

The impact of the crop mask is more complex. It acts to cool the water column for all concentrations of CO_2, with a greater impact in surface waters at high CO_2 concentrations. Despite a smaller cooling impact at 1x CO_2 there is an apparent reduction in stratification of the water column that is not apparent at higher CO_2. Salinity anomalies show more of a complex pattern depending on the CO_2 concentration. At 1x there is an increase in salinity in surface waters and an opposing pattern seen at depth, again reflecting a decrease in stratification. In contrast, the anomaly at 2x, 3x and 4x shows a decrease in surface salinity that extends throughout the water column, particularly at 2x and 4x.

The driver behind the conflicting pattern LUC has on salinity depending on the CO_2 concentration remains uncertain. Maps showing the anomalies in the precipitation/evaporation balance in the Arctic and subtropical gyre (not shown) show no significant change for the LUC simulations compared to the base runs. Instead, changes in sea-ice and surface run-off may play a role, although it remains uncertain as to their relative importance. There is a positive anomaly in surface run-off over much of Western Europe due to LUC (Fig. 9), which may impact GIN Sea salinity. A salinity budget analysis would help clarify the differing roles of such inputs, however this was not possible in this study due to limitations in model output. For 1xLU, cooler and more saline conditions act to slightly increase density and decrease stratification in the water column. For 2xLU and 4xLU however, the potential for cooler temperatures to increase density are likely reversed by the apparent decrease in salinity, resulting in a small reduction in density particularly in surface waters, whilst the density anomaly at 3xLU is negligible. This conflicting pattern of temperature and salinity highlights the complex nature by which density is determined in the GIN Sea.

4 The sensitivity of the AMOC to CO_2 and vegetation

The impact of CO_2, LUC and noLCC on the strength and structure of the AMOC is shown in Figs. 6 and 7. Figure 6 shows the anomalies for the AMOC streamfunction and Fig. 7 a scatter plot of the mean strength and standard deviation of the AMOC MOI (see Fig. 3 for timeseries).

At 1x CO_2 the AMOC has a mean annual strength of 16.6 Sv (1 Sv = $10^6/m^3s^{-1}$) and standard deviation of 1.1 Sv. The strength compares favourably to the 16.9 Sv determined from the RAPID-MOCHA array (16.9 Sv) (Smeed et al. 2015), however it exhibits weaker variability (4.4 Sv) and is too shallow (see Sect. 2).

4.1 The impact of CO_2 on the AMOC

The impact of CO_2 on the strength of the AMOC has been discussed in numerous past studies and is commonly linked to a reduction in density regions of convection driven by a change in the freshwater flux and/or surface heat loss (Dixon et al. 1999; Mikolajewicz and Voss 2000; e.g.; Thorpe et al. 2001; Gregory et al. 2005; Swingedouw et al. 2007).

The response of the AMOC to higher CO_2 in HadCM3 has been discussed in a number of past studies (Armstrong et al. 2017; Thorpe et al. 2001; Thorpe 2005). The AMOC weakens and shallows up to a maximum of 5.0 Sv (30.2%), 4.95 Sv (29.8%) and 5.6 Sv (34%) in the North Atlantic Deep Water (NADW) cell at 2x, 3x and 4x CO_2 respectively (Fig. 6). This is likely a response to the decrease in density as shown in Fig. 5. Thorpe et al. (2001) and Thorpe (2005) used HadCM3 to investigate CO_2-induced weakening of the AMOC and concluded that temperature is a more prominent driver than salinity in reducing density in the GIN Seas, accounting for 60% of AMOC weakening.

4.2 The Impact of LUC and LCC on the AMOC

The AMOC anomaly for 4x_1xVEG (i.e. the anomaly due to the exclusion of LCC) shows an increase in the strength of the AMOC on the order of 4.51 Sv in the NADW cell and approximately 0.43 Sv in the Antarctic Bottom Water (AABW) cell (Fig. 6). The mean AMOC MOI, which is an average value between 40°–50°N at a depth of 800 m, has increased by 2.01 Sv (or +15.06%), resulting in a stronger mean MOI than that for the base 3x CO_2 simulation (Fig. 7). This shows that the inclusion of a dynamic vegetation scheme in a model (i.e. for the 4x simulation) acts to decrease the strength of the AMOC at higher CO_2. Indeed there is a 21% weakening in the AMOC MOI between the 1x and 4x simulations, likely predominantly due to warming as shown in Fig. 5, which is reduced to 6% when vegetation cannot dynamically evolve. There is a subsequent deepening in the NADW cell as shown in Fig. 6. This enhancement is focused in the region of greatest downwelling at approximately 50°N reflecting an increase in GIN Sea density (Fig. 5), deepening in the thermocline and expansion of the mixed layer depth (Fig. 4).

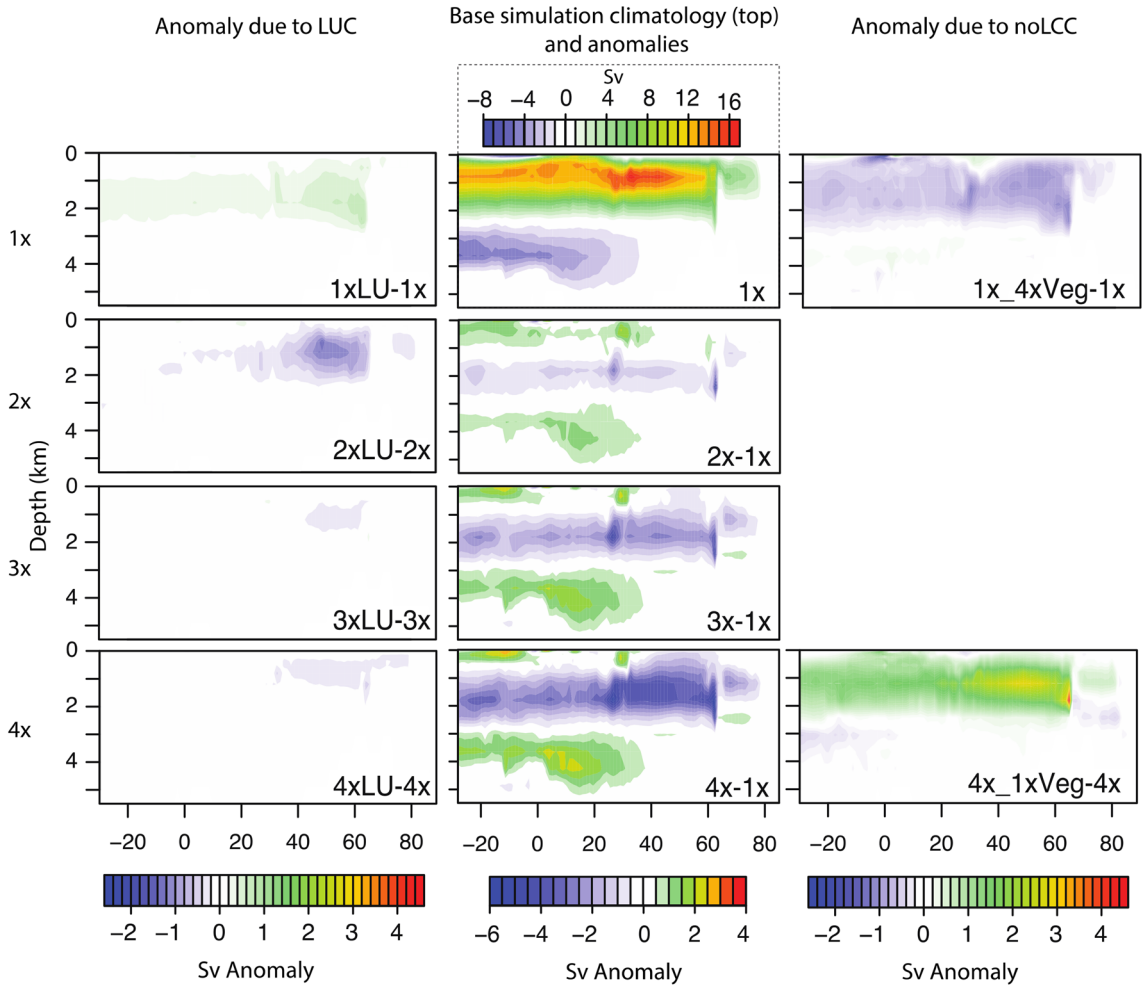

Fig. 6 The mean AMOC streamfunction (Sv) at 1x CO_2 (central top panel) and the anomalies at increasing CO_2 concentrations from top to bottom. The base simulations are shown in the central panels, LUC in the left panels and noLCC in the right panels. Anomalies are calculated from the final 1000 years of each simulation

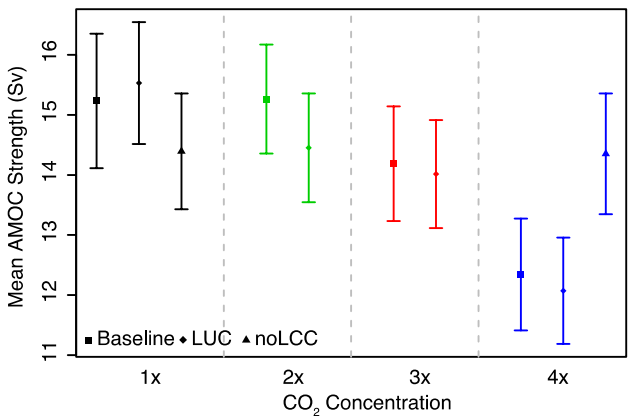

Fig. 7 Scatter plot showing the mean strength and standard deviation (Sv) of the AMOC MOI for the base, LUC and noLCC simulations. The concentration of CO_2 is shown on the x-axis. The MOI is defined as the mean strength of the AMOC between 40-50°N at 800 m for the final 1000 years of each simulation

In contrast, at 1x_4xVEG there is a basin-wide decline in AMOC strength of up to 1.13 Sv in the NADW cell and a reduction in the mean MOI by 0.85 Sv (or −5.67%). The AMOC is also shown to shallow (Fig. 6) although there is no apparent weakening in the AABW cell. This weakening is likely to reflect the decrease in density in the water column (Fig. 5), which shallows the mixed layer depth (Fig. 4).

LUC has a small impact on the strength of the AMOC compared to LCC, likely reflecting the smaller impact that LUC has on the depth profiles of density in the GIN Seas (Fig. 5). At 1x, LUC acts to increase the strength of the MOI by 0.30 Sv (or +1.95%), and weaken the MOI at 2x, 3x, and 4x by −0.81 Sv (−5.45%), −0.17 (−1.20%), −0.27 (−2.21%) respectively. However when applying 95% confidence to the AMOC streamfunctions (not shown), there appears to be no statistically significant change in the strength of the AMOC with LUC.

The contrasting pattern and weaker impact of the crop mask may reflect two factors; at 1x CO_2 the GIN Seas temperature and salinity anomalies are small and so there is only a small increase in GIN Seas density. At 2x, 3x, and 4x CO_2 concentrations, the cooling impact of crops is countered by a decrease in salinity so the impact on GIN Seas density is again small.

The study of Armstrong et al. (2017) highlighted the importance of convection in determining the strength of the AMOC in HadCM3. Figure 8 shows the Brunt-Väisälä (BV) frequency anomalies averaged over the top 666 m for the base and vegetation simulations. High values indicate a greater density gradient, a more stable water column and so reduced convection. The degree of stability in the GIN Seas region increases at higher CO_2, reflecting a more stratified water column and so reduced convection. At 4x_1xVEG there is a predominant negative anomaly across the GIN Seas indicating an increase in convection, potentially linked to a stronger AMOC. This highlights the decrease in stratification in the top 666 m of the water column as shown in Fig. 5, which is likely to be predominantly driven by the decrease in temperatures as salinity shows a contrasting response. In the central part of the basin however there is an area of positive BV frequency that correlates to a region of shallowing in the MLD in Fig. 4. This may indicate a potential southward shift in the position of greatest downwelling at 4x_1xVEG. There is negligible change in GIN Seas stability with the addition of the crop mask.

The apparent sensitivity of the AMOC to LCC indicates that the CO_2 induced shift in vegetation contributes to the decline in the strength of the AMOC in HadCM3. This is likely to be predominantly driven by the indirect biogeophysical impacts of LCC, such as albedo, on temperature. Dynamic vegetation therefore acts to enhance AMOC decline to a greater extent than if vegetation was static and not able to evolve. The inclusion of LUC however has a minimal impact on AMOC strength. This has implications for future research that investigates AMOC sensitivity in HadCM3; highlighting the importance of including a dynamic vegetation scheme. Furthermore this may have implications for other models investigating the AMOC that are included in CMIP6 that have previously not incorporated a DGVM. This will be discussed in more detail in the discussion.

As we have discussed, temperature may be the predominant driver of the changes in AMOC strength that we see for the noLCC simulations. However, for the LUC simulations, salinity may play a more prominent role and may either attenuate or amplifying temperature anomalies. This in part may be influenced by changes in surface runoff (Fig. 9). The LUC runoff anomaly shows an increase in surface runoff focused in regions of significant

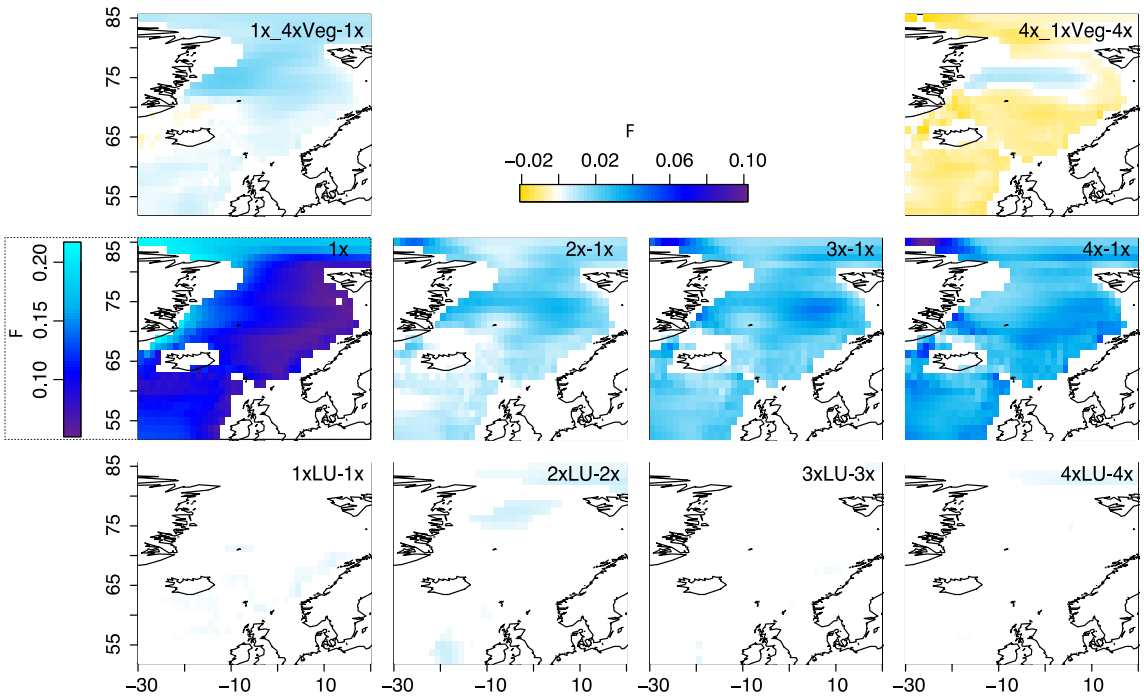

Fig. 8 Brunt-Väisälä (or buoyancy) frequency in the GIN seas for the top 666 m at 1x CO_2 (middle left panel) and anomalies due to increasing CO_2 at 2x, 3x and 4x (middle panels), LUC (bottom panels) and noLCC (top panels). The simulations used to calculate each plot is shown in each panel. High values indicate a more stable water column and thus reduced convection. Only anomalies that are considered 95% confident are shown

LUC, primarily reflecting the replacement of vegetation with grasses and an increase in throughfall. Anomalies are more heavily focused around the GIN Seas, the key region of convection, due to crop conversion in Western Europe. These might impact GIN Seas salinity, and may be responsible for driving the negative salinity anomalies apparent at 2x, 3x and 4x CO_2. For the noLCC simulations the effect around the GIN Seas is small, which may indicate that surface runoff does not have a significant impact in these simulations. Further simulations are required that include a range of diagnostics to perform a salinity budget analysis or controlling for surface run-off in their set-up. This would permit identification of the direct and indirect inputs, how these influence the AMOC, and how they are altered for the different simulations.

5 The impact of the AMOC on vegetation

Above we have discussed how LUC/LCC influences AMOC strength, but it also worth considering the sensitivity of vegetation simulated by a DGVM to small internal fluctuations in AMOC strength simulated by HadCM3. In Fig. 3, it is apparent that the AMOC fluctuates in strength throughout the simulations, the timescales and mechanisms of which are discussed in detail in Armstrong et al. (2017). A number of past studies have linked vegetation change to fluctuations in the strength of the AMOC, via both pollen records (Grimm et al. 2006; Fletcher et al. 2010; Allen et al. 1999), ocean cores (Fletcher and Goni 2008; Nebout et al. 2009) and in modelling studies (Kohler et al. 2005; Scholze et al. 2003; Menviel et al. 2008). Such studies have predominantly focused on how vegetation responds to a forced collapse or abrupt change in the AMOC, such as that expected from the DO and HE events (e.g. Kohler et al. 2005; Scholze et al. 2003; Menviel et al. 2008; Woillez et al. 2013) and in turn how this may be linked to pollen records. Here we will investigate whether there is such a response to small internal fluctuations in AMOC strength simulated by HadCM3.

Figures 10 and 11 shows the no lag correlations of the AMOC Index (MOI) with the different PFTs and the associated net primary productivity (NPP) for the base simulations. Positive anomalies indicate an increase in the vegetation type or NPP with the MOI and vice versa. Despite the small changes in AMOC strength, there are apparent regional relationships of vegetation change with the AMOC. At 1x CO_2, there is an apparent increase in C4 grasses and decrease in shrubs and C3 grasses across much of central North America and areas of south subtropical Africa. Across Western Europe there is an apparent reduction in C3 grasses and bare soil with a potential increase in shrubs. Broadleaf trees decrease across areas of the Amazon and southern subtropical Africa. Correlations at both 2x and 3x are weaker and more spatially intermittent. At 4x there appears to be a positive relationship with broadleaf trees across Canada in place of needleleaf and a negative relationship with broadleaf in southern South America. The response of vegetation type would be expected to lag behind changes in the AMOC, however NPP is likely to respond more rapidly. At 1x, Fig. 11 shows a potentially positive correlation in the NPP of broadleaf trees and C4 grasses across Eurasia, and a negative correlation in shrubs and needleleaf trees across

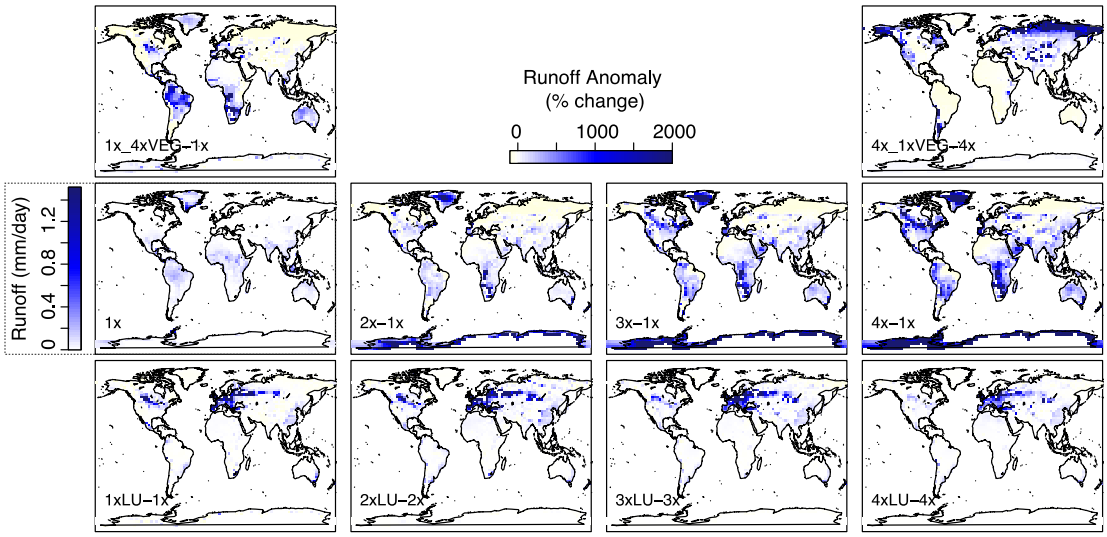

Fig. 9 Surface run-off anomalies. Mean annual climatology at 1x CO_2 (left central map) and anomalies due to CO_2 in the central panels, LUC (i.e. the conversion of natural vegetation to crops) in the lower panels and noLCC in the top panels. Only anomalies that are considered 95% confident are shown

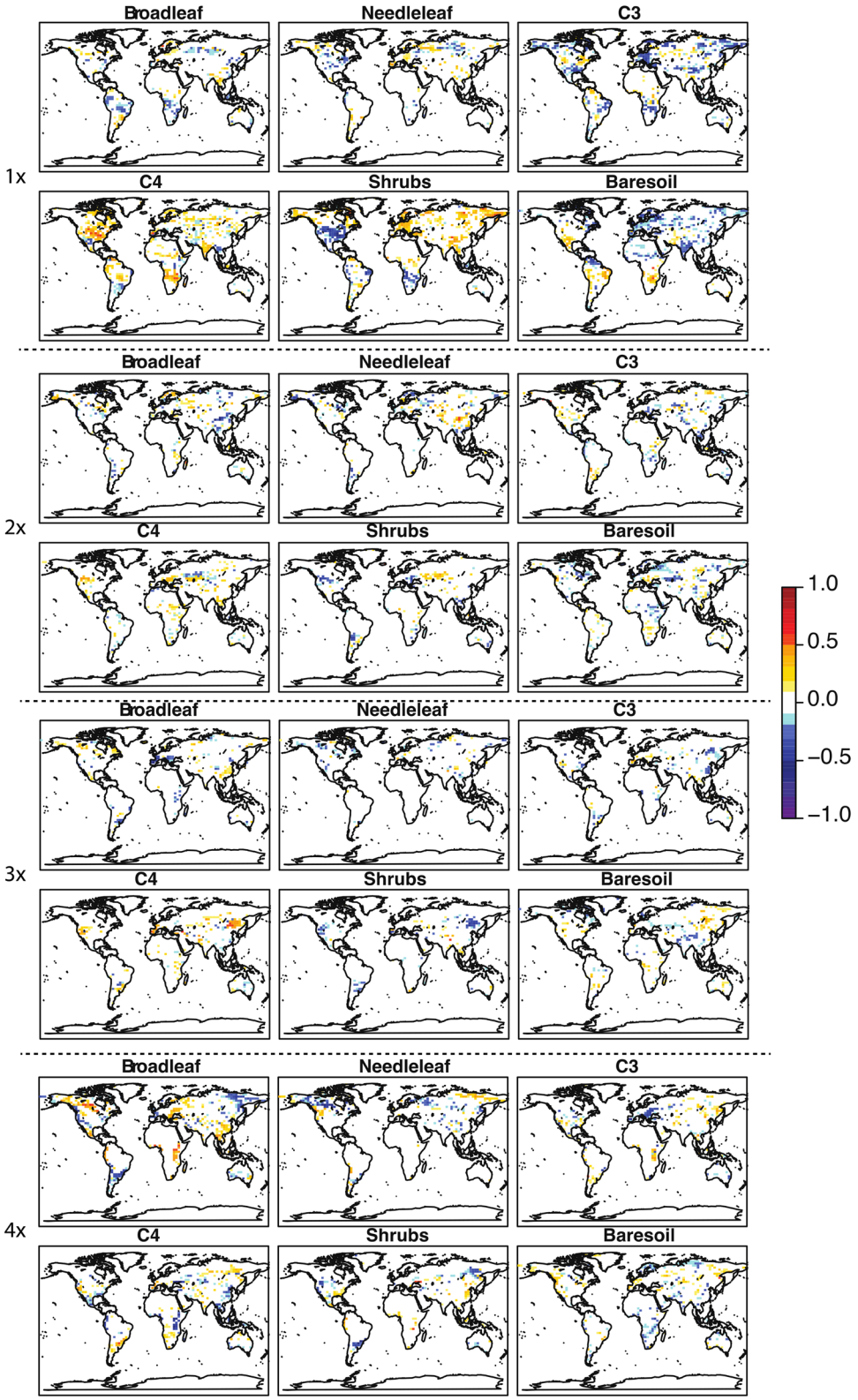

Fig. 10 No lag correlation of PFTs simulated by TRIFFID with the MOI for the base simulations; 1x, 2x, 3x and 4x (top to bottom). The MOIs for the base simulations are shown in Fig. 3 and the final 1000 years used. Only anomalies that are considered 95% confident are shown

North America. Similarly to vegetation distribution, there is an apparent decline in these correlations at higher CO_2 concentrations.

Although Figs. 10 and 11 indicate statistically significant correlations between vegetation and NPP with the AMOC, they do not give an indication as to the extent of vegetation or NPP change. Figure 12 shows the mean annual proportion

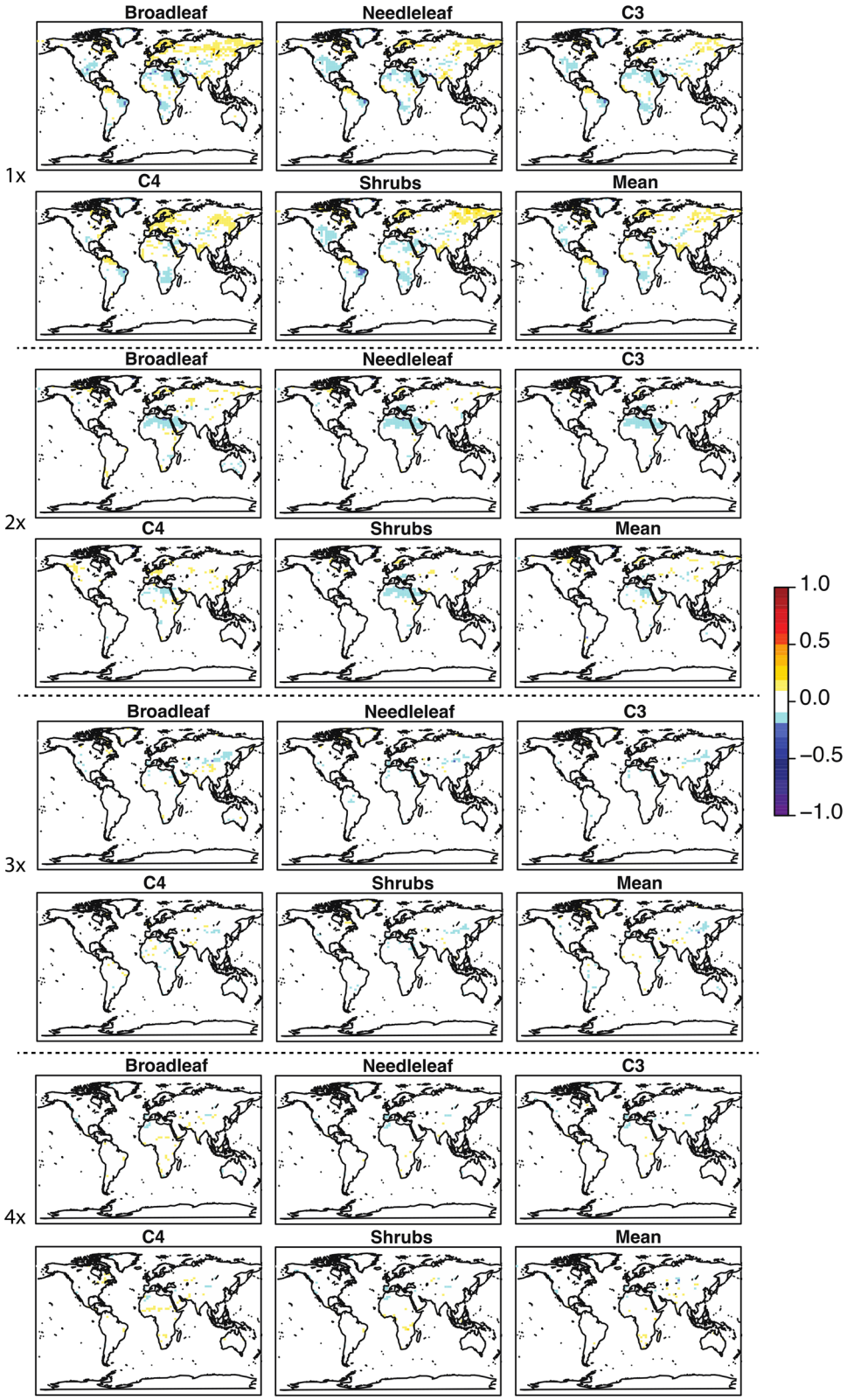

Fig. 11 No lag correlation of net primary productivity (NPP) for each of the PFTs with the MOI for the base simulations; 1x, 2x, 3x and 4x (top to bottom). The MOIs for the base simulations are shown in Fig. 3 and the final 1000 years used. Only anomalies that are considered 95% confident are shown

of a PFT and associated NPP for a specific region against the mean annual strength of the AMOC at 1x CO_2. Here each point represents one simulation year (1000 in total) with a simple linear regression line of best fit demonstrating the trend for both PFT (red line) and NPP (green line). Despite the apparent correlation relationships in Figs. 10 and 11, the

actual proportional change in vegetation type and NPP with the AMOC is small, often on the order of between 1 and 2% when considering vegetation change. Furthermore the relationships are generally weak and hindered by significant interannual variation irrespective of AMOC change, particularly for bare soil.

Despite this there are some apparent trends, including an increase in the proportion and NPP of shrubs across Europe that may reflect the increase in precipitation that occurs during periods of maximum AMOC (see Armstrong et al. 2017). This may reflect a northward shift in the position of the ITCZ due to an increased equatorial sea surface gradient during these periods and therefore an increase in precipitation. Within TRIFFID, increased precipitation would favour the growth of shrubs in place of grasses, which are higher in the hierarchal methodology (i.e. trees > shrubs > grasses). In North America there is a decline in the proportion and NPP of shrubs, which in contrast may reflect the modelled reduction in precipitation during periods of strong AMOC. There is a decline in the extent and NPP of C3 grasses across Southern Africa potentially reflecting a decrease in precipitation and consequent increase in C4 grasses.

The limited impact of the AMOC on simulated vegetation distribution and NPP is likely to reflect the relatively small changes in precipitation and temperatures during periods of strong and weak AMOC (not shown). In Western Europe, temperature and precipitation anomalies are on the order of 0.5 °C and 0.1 mm/day respectively. In contrast, the study of Woillez et al. (2013) who used IPSL to investigate vegetation response to AMOC collapse had climatic changes of approximately 1.7 °C and 0.35 mm/day in precipitation over Western Europe, which consequently resulted in the replacement of trees with shrubs and grasses across much of the region. The small climatic changes in HadCM3 due to internal AMOC variability would be expected to instigate only a small change in vegetation type and NPP, and likely only to those in areas that are close to a climate threshold. Furthermore the role of vegetation-dependent timescales might also be important with regards to changes in distribution, with trees expected to show less of a signal than grasses and shrubs due to there longer response time. This is likely to be the case where climate change is positive for growth, however in regions where the climate response is negative then they can potentially die off quickly. It is also worth noting here that AMOC variability in HadCM3 has a standard deviation (SD) of 1.1 Sv at 1x CO_2, which is smaller than the 4.4 Sv simulated by the RAPID-MOCHA array (Smeed et al. 2015). The vegetation response to the AMOC in the real climate system might therefore be more significant, further experiments would be required to test this.

6 Discussion and conclusions

This study has used the HadCM3 coupled climate model run for millennial timescales to investigate the sensitivity of the AMOC to vegetation at four equilibrium CO_2 concentrations; 350, 700, 1050 and 1400 ppm (1x, 2x, 3x and 4x respectively). The impact of vegetation has been investigated in two ways; firstly the response of the AMOC to the 'background' vegetation state dynamically simulated by the DGVM TRIFFID that is altered at higher CO_2, here referred to as land cover change (LCC). A set of simulations is run without LCC included, termed noLCC,

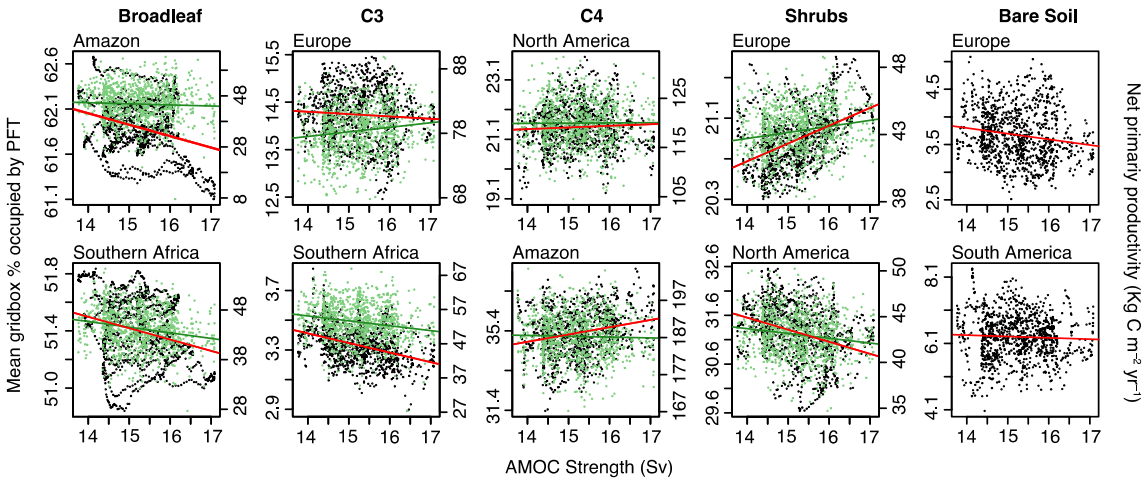

Fig. 12 Mean annual proportion of PFTs (% grid square) and NPP (Kg C m^{-2} $year^{-1}$) for specific regions vs. the mean annual AMOC strength determined from the SSA MOI at 1x CO_2. Different PFTs are shown in each column. The red line shows the line of best fit for PFT proportion and the green line for NPP calculated by linear regression. The regions are defined as; North America 17.5°N–72.5°N:161.25°W–56.25°W, South America −55°S–10°N:82.5°W–37.5°W, Europe 37.5°N–70°N:15°W–37.5°E, Africa −32.5°S–35°N:15°W–37.5°E

in order to investigate the impact this has. Secondly the influence of agriculture is investigated by using a crop/pasture mask that represents the global disturbed fraction as of the year 1990 (Betts et al. 2007), referred to here as land-use change (LUC). The key findings are:

- Increasing CO_2 acts to weaken the AMOC, a response to an increase in buoyancy in the Greenland-Iceland-Norwegian Seas (GIN Seas) due to elevated temperatures and a change in salinity. This, in addition to an increase in stratification, decreases convection and consequently AMOC strength.
- The change in LCC simulated at higher concentrations of CO_2 acts to amplify warming across much of the Northern Hemisphere, likely due to a reduction in albedo reflecting the predominant replacement of grasses/shrubs with forest at high latitudes.
- The in-direct climatological impacts of LCC, e.g. the impact it has on biogeophysical properties such as albedo which subsequently affects temperature, influences the GIN Seas region; decreasing surface density, increasing stratification and weakening convection.
- LCC consequently acts to weaken the AMOC. At 4xCO_2, dynamic vegetation enhances AMOC decline from 6 to 21%.
- LUC cools climate over regions of high crop fraction. However the impact on density and convection in the GIN Seas are small, potentially due to opposing temperature and salinity anomalies. Salinity anomalies might be influenced by an increase in surface runoff due to changing vegetation distribution, although further simulations are required to test this.
- Consequently LUC has negligible impact on AMOC strength
- As with the base simulations, increasing CO_2 for the LUC and noLCC simulations is associated with an overall decline in AMOC strength.
- The AMOC fluctuates in strength throughout the simulation, showing a standard deviation of 1.1 Sv at 1x CO_2. This has a small but statistically significant impact on regional vegetation distributions and NPP.

These results show that a dynamic vegetation scheme impacts the AMOC in a climate model. The impact on LUC however appears to be small. This may have implications for predicting the AMOC in future climate projections using both HadCM3 and potentially other climate models used in CMIP5 and the upcoming CMIP6 (Eyring et al. 2016).

Despite the potential importance of a dynamic vegetation scheme in modelling the AMOC, only 3 of almost 40 models included in CMIP5 included a dynamic vegetation component; MIROC, MPI and HadGEM. This small number makes it difficult to put this research into context with other models. Reintges et al. (2017) concluded that model uncertainty (rather than scenario or internal) was the most crucial factor that influenced projections of the AMOC in CMIP5 models, regardless of vegetation distribution. This uncertainty is primarily associated with the ocean, atmosphere, and sea-ice components, which influence the fluxes of heat, momentum and freshwater which consequently impact the AMOC. The factors that determine the density of the water column, i.e. temperature and more importantly salinity, are crucial in influencing the AMOC. These vary significantly both spatially and temporally between models. This is reflected in the large spread of AMOC strength and projections in CMIP5 studies. Reintges et al. (2017) showed that the spread in AMOC strength for 32 of the CMIP5 models is large, with the vertical maximum strength at 26.5°N ranging from 12.1 Sv to 29.7 Sv. Cheng et al. (2013) analysed the trend of the AMOC MOI (max transport at 30°N) in 10 of the CMIP5 models up to the year 2100 for the RCP4.5 and RCP8.5 scenarios, concluding that the decline in AMOC strength ranged from 5 to 40% and 15–60% respectively. This is compared to a decline of 34% when quadrupling CO_2 (i.e. 1400 ppm) in HadCM3 with the addition of dynamic vegetation. Although the results shown here cannot be directly compared with those presented in these studies, they are indicative of the wide range of uncertainty within models even before the introduction of additional uncertainty associated with a DGVM.

Further to this, the feedbacks associated with dynamic vegetation are likely to be highly model dependant, with those identified in HadCM3 unlikely to be similarly reflected in other models. It is particularly problematic that the direct impacts of LUC/LCC (i.e. runoff) cannot be differentiated from the in-direct impacts, which are more a response to vegetation distribution rather than model climatology. The impact of LUC also shows significant model disparity as to the magnitude and even direction of effects (Pitman et al. 2009; de Noblet-Ducoudre et al. 2012; Brovkin et al. 2013), reflecting inconsistencies between model parameterisations.

The large spread in model output, with or without a DGVM, indicates that the importance of including vegetation may be overshadowed by other systemic model biases. The priority for the modelling community is likely to focus on the narrowing of this uncertainty band before the introduction of a DGVM that introduces further climate biases into the system. However, the results here do indicate that a dynamic vegetation scheme may have a relatively significant impact in models, and should therefore be considered as an important component of the model set-up. At the very least, future work should focus on the feedbacks between vegetation and the AMOC in a range of other climate models.

Acknowledgements This work was funded by the U.K. National Environmental Research Council (NERC) Grant NE/L501554/1. Climate simulations were carried out using the computational facilities of the Advanced Computing Research Centre, University of Bristol (http://www.bris.ac.uk/acrc) (Bluecrystal). Our thanks go the helpful advice of an anonymous reviewer.

References

Allen JRM, Brandt U, Brauer A, Hubberten HW, Huntley B, Keller J, Kraml M, Mackensen A, Mingram J, Negendank JFW, Nowaczyk NR, Oberhansli H, Watts WA, Wulf S, Zolitschka B (1999) Rapid environmental changes in southern Europe during the last glacial period. Nature 400:740–743

Armstrong E, Valdes PJ, House J, Singarayer JS (2016) The role of CO_2 and dynamic vegetation on the impact of temperate land use change in the HadCM3 coupled climate model. Earth Interact 20:1–20

Armstrong E, Valdes P, House J, Singarayer J (2017) Investigating the impact of CO_2 on low-frequency variability of the AMOC in HadCM3. J Clim 30:7863–7883

Bakker P, Schmittner A, Lenaerts J, Abe-Ouchi A, Bi D, van den Broeke MR, Chan W-L, Hu A, Beadling RL, Marsland SJ, Mernild SH, Saenko OA, Swingedouw D, Sullivan A, Yin J (2016) Fate of the Atlantic Meridional overturning circulation: strong decline under continued warming and Greenland melting. Geophys Res Lett 43:12252–12260

Bala G, Caldeira K, Wickett M, Phillips TJ, Lobell DB, Delire C, Mirin A (2007) Combined climate and carbon-cycle effects of large-scale deforestation. Proc Natl Acad Sci USA 104:6550–6555

Bathiany S, Claussen M, Brovkin V, Raddatz T, Gayler V (2010) Combined biogeophysical and biogeochemical effects of large-scale forest cover changes in the MPI earth system model. Biogeosciences 7:1383–1399

Betts RA, Cox PM, Collins M, Harris PP, Huntingford C, Jones CD (2004) The role of ecosystem-atmosphere interactions in simulated Amazonian precipitation decrease and forest dieback under global climate warming. Theoret Appl Climatol 78:157–175

Betts RA, Falloon PD, Goldewijk KK, Ramankutty N (2007) Biogeophysical effects of land use on climate: Model simulations of radiative forcing and large-scale temperature change. Agric For Meteorol 142:216–233

Boisier JP, de Noblet-Ducoudre N, Pitman AJ, Cruz FT, Delire C, van den Hurk BJJM, van der Molen MK, Muller C, Voldoire A (2012) Attributing the impacts of land-cover changes in temperate regions on surface temperature and heat fluxes to specific causes: results from the first LUCID set of simulations. J Geophys Res-Atmos. 117:D12

Bonan GB (2001) Observational evidence for reduction of daily maximum temperature by croplands in the Midwest United States. J Clim 14:2430–2442

Brovkin V, Raddatz T, Reick CH, Claussen M, Gayler V (2009) Global biogeophysical interactions between forest and climate. Geophys Res Lett 36:L07405

Brovkin V, Boysen L, Arora VK, Boisier JP, Cadule P, Chini L, Claussen M, Friedlingstein P, Gayler V, van den Hurk BJJM, Hurtt GC, Jones CD, Kato E, de Noblet-Ducoudre N, Pacifico F, Pongratz J, Weiss M (2013) Effect of anthropogenic land-use and land-cover changes on climate and land carbon storage in CMIP5 projections for the twenty-first century. J Clim 26:6859–6881

Cattle H, Cresswell D (2000) The Arctic Ocean freshwater budget of a climate general circulation model. Freshw Budg Arct Ocean 70:127–139

Cheng W, Chiang JCH, Zhang DX (2013) Atlantic meridional overturning circulation (AMOC) in CMIP5 models: RCP and historical simulations. J Clim 26:7187–7197

Claussen M, Brovkin V, Ganopolski A (2001) Biogeophysical versus biogeochemical feedbacks of large-scale land cover change. Geophys Res Lett 28:1011–1014

Cox P (2001) Description of the 'TRIFFID' dynamic global vegetation model. Technical Report 24. Hadley Centre Met Office, Devon

de Noblet-Ducoudre N, Boisier JP, Pitman A, Bonan GB, Brovkin V, Cruz F, Delire C, Gayler V, van den Hurk BJJM, Lawrence PJ, van der Molen MK, Muller C, Reick CH, Strengers BJ, Voldoire A (2012) Determining robust impacts of land-use-induced land cover changes on surface climate over North America and Eurasia: results from the first set of LUCID experiments. J Clim 25:3261–3281

Dixon KW, Delworth TL, Spelman MJ, Stouffer RJ (1999) The influence of transient surface fluxes on North Atlantic overturning in a coupled GCM climate change experiment. Geophys Res Lett 26:2749–2752

Essery RLH, Best MJ, Betts RA, Cox PM, Taylor CM (2003) Explicit representation of subgrid heterogeneity in a GCM land surface scheme. J Hydrometeorol 4:530–543

Eyring V, Bony S, Meehl GA, Senior CA, Stevens B, Stouffer RJ, Taylor KE (2016) Overview of the Coupled Model Intercomparison Project Phase 6 (CMIP6) experimental design and organization. Geosci Model Dev 9:1937–1958

Flato G, Marotzke J, Abiodun B, Braconnot P, Chou SC, Collins W, Cox P, Driouech F, Emori S, Eyring V, Forest C, Gleckler P, Guilyardi E, Jakob C, Kattsov V, Reason C, Rummukainen M (2013) Evaluation of climate models. In: Stocker TF, Qin D, Plattner G-K, Tignor M, Allen SK, Boschung J, Nauels A, Xia Y, Bex V, Midgley PM (eds) Climate change 2013: the physical science basis. Contribution of working group I to the fifth assessment report of the intergovernmental panel on climate change. Cambridge University Press, Cambridge and New York, pp 741–866

Fletcher WJ, Goni MFS (2008) Orbital- and sub-orbital-scale climate impacts on vegetation of the western Mediterranean basin over the last 48,000 year. Quatern Res 70:451–464

Fletcher WJ, Goni MFS, Allen JRM, Cheddadi R, Combourieu-Nebout N, Huntley B, Lawson I, Londeix L, Magri D, Margari V, Muller UC, Naughton F, Novenko E, Roucoux K, Tzedakis PC (2010) Millennial-scale variability during the last glacial in vegetation records from Europe. Quatern Sci Rev 29:2839–2864

Ge J (2010) MODIS observed impacts of intensive agriculture on surface temperature in the southern Great Plains. Int J Climatol 30:1994–2003

Goldewijk KK (2001) Estimating global land use change over the past 300 years: The HYDE Database. Global Biogeochem Cycles 15:417–433

Gordon C, Cooper C, Senior CA, Banks H, Gregory JM, Johns TC, Mitchell JFB, Wood RA (2000) The simulation of SST, sea ice extents and ocean heat transports in a version of the Hadley Centre coupled model without flux adjustments. Clim Dyn 16:147–168

Gregory JM, Dixon KW, Stouffer RJ, Weaver AJ, Driesschaert E, Eby M, Fichefet T, Hasumi H, Hu A, Jungclaus JH, Kamenkovich IV, Levermann A, Montoya M, Murakami S, Nawrath S, Oka A, Sokolov AP, Thorpe RB (2005) A model intercomparison of changes in the Atlantic thermohaline circulation in response to

increasing atmospheric CO_2 concentration. Geophys Res Lett 32:L12703
Grimm EC, Watts WA, Jacobson GL, Hansen BCS, Almquist HR, Dieffenbacher-Krall AC (2006) Evidence for warm wet Heinrich events in Florida. Quatern Sci Rev 25:2197–2211
Hall P (1988) Theoretical comparison of bootstrap confidence-intervals. Ann Stat 16:927–953
Hawkins E, Sutton R (2007) Variability of the Atlantic thermohaline circulation described by three-dimensional empirical orthogonal functions. Clim Dyn 29:745–762
Hu AX, Meehl GA (2005) Bering strait throughflow and the thermohaline circulation. Geophys Res Lett 32:L24610
Jackson L, Vellinga M (2013) Multidecadal to centennial variability of the AMOC: HadCM3 and a perturbed physics ensemble. J Clim 26:2390–2407
Jiang DB, Zhang Y, Lang XM (2011) Vegetation feedback under future global warming. Theoret Appl Climatol 106:211–227
Kohler P, Joos F, Gerber S, Knutti R (2005) Simulated changes in vegetation distribution, land carbon storage, and atmospheric CO_2 in response to a collapse of the North Atlantic thermohaline circulation. Clim Dyn 25:689–708
Manabe S, Stouffer RJ (1980) Sensitivity of a global climate model to an increase of CO_2 concentration in the atmosphere. J Geophys Res-Oceans Atmos 85:5529–5554
Meinshausen M, Smith SJ, Calvin K, Daniel JS, Kainuma MLT, Lamarque JF, Matsumoto K, Montzka SA, Raper SCB, Riahi K, Thomson A, Velders GJM, van Vuuren DPP (2011) The RCP greenhouse gas concentrations and their extensions from 1765 to 2300. Clim Chang 109:213–241
Menviel L, Timmermann A, Mouchet A, Timm O (2008) Meridional reorganizations of marine and terrestrial productivity during Heinrich events. Paleoceanography 23:PA1203
Mikolajewicz U, Voss R (2000) The role of the individual air-sea flux components in CO_2-induced changes of the ocean's circulation and climate. Clim Dyn 16:627–642
Nebout NC, Peyron O, Dormoy I, Desprat S, Beaudouin C, Kotthoff U, Marret F (2009) Rapid climatic variability in the west Mediterranean during the last 25000 years from high resolution pollen data. Clim Past 5:503–521
Pielke RA, Marland G, Betts RA, Chase TN, Eastman JL, Niles JO, Niyogi DDS, Running SW (2002) The influence of land-use change and landscape dynamics on the climate system: relevance to climate-change policy beyond the radiative effect of greenhouse gases. Philos Trans R Soc Lond Ser Math Phys Eng Sci 360:1705–1719
Pitman AJ, de Noblet-Ducoudre N, Cruz FT, Davin EL, Bonan GB, Brovkin V, Claussen M, Delire C, Ganzeveld L, Gayler V, van den Hurk BJJM, Lawrence PJ, van der Molen MK, Muller C, Reick CH, Seneviratne SI, Strengers BJ, Voldoire A (2009) Uncertainties in climate responses to past land cover change: first results from the LUCID intercomparison study. Geophys Res Lett 36:L14814
Pope VD, Gallani ML, Rowntree PR, Stratton RA (2000) The impact of new physical parametrizations in the Hadley Centre climate model: HadAM3. Clim Dyn 16:123–146
Ramankutty N, Foley JA (1999) Estimating historical changes in global land cover: croplands from 1700 to 1992. Global Biogeochem Cycles 13:997–1027
Reintges A, Martin T, Latif M, Keenlyside NS (2017) Uncertainty in twenty–first century projections of the Atlantic Meridional overturning circulation in CMIP3 and CMIP5 models. Clim Dyn 49 1–17
Roberts MJ, Marsh R, New AL, Wood RA (1996) An intercomparison of a Bryan-Cox-type ocean model and an isopycnic ocean model. 1. The subpolar gyre and high-latitude processes. J Phys Oceanogr 26:1495–1527
Scholze M, Knorr W, Heimann M (2003) Modelling terrestrial vegetation dynamics and carbon cycling for an abrupt climatic change event. Holocene 13:327–333
Singarayer JS, Davies-Barnard T (2012) Regional climate change mitigation with crops: context and assessment. Philos Trans Ser A Math Phys Eng Sci 370:4301–4316
Singarayer JS, Ridgwell A, Irvine P (2009) Assessing the benefits of crop albedo bio-geoengineering. Environ Res Lett 4:045110
Smeed D, McCarthy G, Rayner D, Moat BI, Johns WE, Baringer M, Meinen CS (2015) Atlantic meridional overturning circulation observed by the RAPID-MOCHA-WBTS (RAPID-Meridional overturning circulation and heatflux array-Western boundary time series) array at 26N from 2004 to 2014. British Oceanographic Data Centre—Natural Environment Research Council, Liverpool
Snyder PK, Delire C, Foley JA (2004) Evaluating the influence of different vegetation biomes on the global climate. Clim Dyn 23:279–302
Swingedouw D, Braconnot P, Delecluse P, Guilyardi E, Marti O (2007) Quantifying the AMOC feedbacks during a 2xCO(2) stabilization experiment with land-ice melting. Clim Dyn 29:521–534
Thorpe R (2005) The impact of changes in atmospheric and land surface physics on the thermohaline circulation response to anthropogenic forcing in HadCM2 and HadCM3. Clim Dyn 24:449–456
Thorpe RB, Gregory JM, Johns TC, Wood RA, Mitchell JFB (2001) Mechanisms determining the Atlantic thermohaline circulation response to greenhouse gas forcing in a non-flux-adjusted coupled climate model. J Clim 14:3102–3116
Valdes PJ, Armstrong E, Badger MPS, Bradshaw C, Bragg F, Davies-Barnard T, Day JJ, Farnsworth A, Hopcroft P, Kennedy A, Lord N, Lunt DJ, Marzocchi A, Parry L, Roberts W, Stone E, Tourte G, Williams J (2017) The BRIDGE HadCM3 family of climate models: HadCM3@Bristol v1.0. Geosci Model Develop 10:3715–3743
Vellinga M, Wu PL (2004) Low-latitude freshwater influence on centennial variability of the Atlantic thermohaline circulation. J Clim 17:4498–4511
Wilks DS (1997) Resampling hypothesis tests for autocorrelated fields. J Clim 10:65–82
Woillez MN, Kageyama M, Combourieu-Nebout N, Krinner G (2013) Simulating the vegetation response in western Europe to abrupt climate changes under glacial background conditions. Biogeosciences 10:1561–1582